

# Discrete Green's function approach to disjoint domain simulations in 3D FDTD method

T.P. Stefański

A discrete Green's function (DGF) approach to couple 3D FDTD subdomains is developed. The total-field/scattered-field subdomains are simulated using the explicit FDTD method whilst interaction between them is computed as a convolution of the DGF with equivalent current sources measured over Huygens surfaces. In the developed method, the DGF waveforms are truncated using the Hann's window. The error varies in the range  $-65$  to  $-40$  dB depending on the DGF length and positions of the subdomains. However, if the DGF length is equal to the number of iterations in a simulation, this approach returns the same results as the direct FDTD method.

**Introduction:** The hybridisation between the finite-difference time-domain (FDTD) method [1] and integral equation based numerical methods requires consistency with the discrete electromagnetism theory and the discrete Green's function (DGF) that is compatible with Yee's grid [2]. The FDTD method and its DGF-based formulation can be perfectly coupled because the DGF is directly derived from the FDTD update equations. Although several attempts at coupling the FDTD method with integral equation based numerical methods have been reported in the literature, these techniques work well until instabilities kick in [3].

Therefore, the objective of this Letter is to demonstrate for the first time a new technique for coupling 3D FDTD subdomains. Stable 2D FDTD simulations on disjoint domains employing the DGF-based boundary condition have already reported [3]. However, up to now, the coupling of FDTD subdomains with use of the DGF has not yet been presented in 3D to the best of the author's knowledge.

**Developed method:** The idea behind the developed method is schematically depicted in Fig. 1, whereas the detailed flowchart of the FDTD method on disjoint domains is presented in Fig. 2.

The presented method was developed for two FDTD subdomains coupled using an integral equation with the DGF kernel. Simulated objects (e.g. source and scatterer) are placed within the FDTD subdomains, which are terminated by the perfectly matched layers (PMLs) [1]. Although the DGF can also provide a global absorbing boundary condition (ABC), the quality of PMLs is sufficient to demonstrate the developed algorithm. Moreover, the computational efficiency of PMLs is much higher than global ABCs.

In the developed method, implementation of Huygens boxes is consistent with the equivalence theorem in the discrete domain [4]. A simulated object within a subdomain is placed inside two Huygens boxes comprising three surfaces separated by a half-cell distance: (i) outer  $S_e$  and  $S_h$  in the scattered-field zone to calculate the field radiated from the subdomain, and (ii) inner  $S_e$  and  $S_h$  for excitation of the total-field/scattered-field (TFSF) boundary [1]. The  $S_e$  and  $S_h$  surfaces of the Huygens boxes respectively correspond to the tangential electric- and magnetic-field components in the Yee's grid. Equivalent currents ( $\mathbf{J}$ ,  $\mathbf{M}$ ) in the scattered-field zone allow computing the field impinging at the coupled subdomain. The incident field ( $\mathbf{E}$ ,  $\mathbf{H}$ ) at the TFSF boundary in the coupled subdomain can be computed as a convolution of the current sources ( $\mathbf{J}$ ,  $\mathbf{M}$ ) and the dyadic DGF [2]:

$$\begin{bmatrix} \mathbf{E}_{ijk}^n \\ \eta \mathbf{H}_{ijk}^n \end{bmatrix} = \sum_{n' i' j' k'} \begin{bmatrix} \mathbf{G}_{ee}^{n-n'} & \mathbf{G}_{eh}^{n-n'} \\ \mathbf{G}_{he}^{n-n'} & \mathbf{G}_{hh}^{n-n'} \end{bmatrix} \begin{bmatrix} c \Delta t \eta \mathbf{J}_{i' j' k'}^{n'} \\ c \Delta t \mathbf{M}_{i' j' k'}^{n'} \end{bmatrix} \quad (1)$$

where  $c$  denotes the speed of light,  $\eta$  is the intrinsic impedance of free space,  $n$  is the time index and  $\Delta t$  is the time-step size.

The coupling of FDTD subdomains requires generation of the DGF waveforms corresponding to the equivalent currents measured over the Huygens surfaces. The DGF generation is a part of the pre-processing stage or, alternatively, the DGF waveforms can be downloaded from the DGF file on a hard drive. In the developed method, the acceleration of the DGF computations on a graphics processing unit was employed [5]. However, the size of available memory and runtime will still limit the feasibility of generation of long DGF waveforms, as well as at the pre-processing stage. If the length of the DGF waveforms is equal to the number of iterations in the FDTD simulation,

the presented technique returns the same results as the direct FDTD method (assuming infinite numerical precision of computations). Since the DGF generation and convolution computations require processor time, the DGF was truncated using the Hann's window [6]:

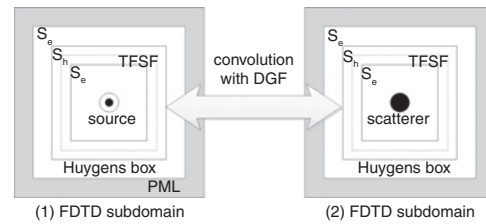


Fig. 1 Implementation of disjoint domain simulations in FDTD method; DGF used to model propagation between subdomains

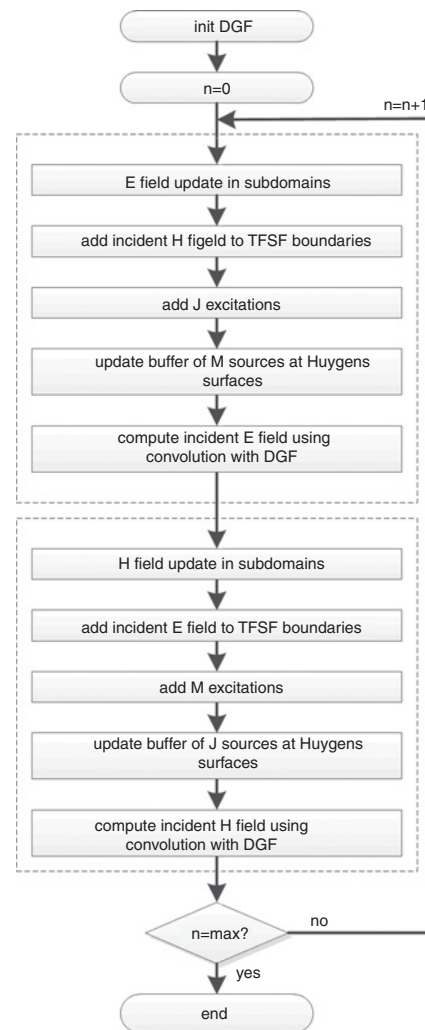
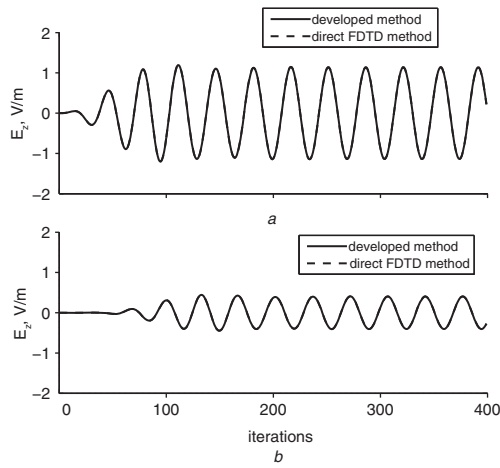
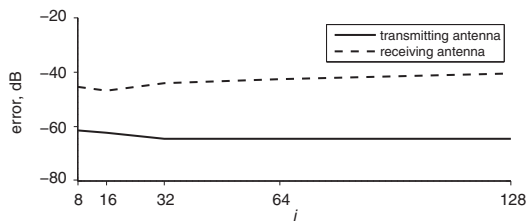


Fig. 2 Flowchart of developed algorithm

**Numerical results:** The method described above was integrated with the 3D FDTD solver. Two half-wavelength dipoles were placed inside subdomains, each with Huygens box of size  $4 \times 4 \times 15$  cells. The spatial discretisation was taken as  $\Delta x = \Delta y = \Delta z = 1$  mm for the results presented here. The harmonic current source (the corresponding wavelength  $\lambda = 20\Delta x$ ) excited the transmitting antenna whereas the electric field was measured by the receiving antenna in the second subdomain. The relative position of both subdomains was varied in the direction  $(i, i, 0)$ , where  $i = 8, 16, 32, 64, 128$ . Exemplary waveforms, compared with the result of the direct FDTD simulation, are presented in Fig. 3. As seen, waveforms computed using both methods overlap. The differences measured between waveforms (defined as in [6]) are presented in Fig. 4.



**Fig. 3** Exemplar waveforms recorded by transmitting antenna (Fig. 3a) and receiving antenna (Fig. 3b); shift between antennas:  $(i, i, 0) = (8, 8, 0)$ , Hann's window length  $n_s = 100$



**Fig. 4** Relative error between waveforms computed using developed method and direct FDTD method for varied position  $(i, i, 0)$  of receiving antenna from transmitting antenna

As reported in [6], application of the windowing technique to truncate the DGF requires a sufficiently long window to guarantee accuracy of computations. For the sake of brevity, the evaluation of the errors resulting from the DGF windowing will not be repeated here.

Runtime scaling of convolution computations executed over  $M$  cells at a single Huygens surface is of order  $(M n_s)$ , where  $n_s$  denotes the DGF length. The runtime scaling is of order  $(M^2 n_s)$  for two coupled subdomains (computational cost of the FDTD updates is neglected). On the other hand, FDTD computations require updating of all cells in the extended domain including both subdomains. Runtime scaling of these computations is of order  $(N^3)$ , where  $N^3$  denotes the number of cells in a cubic FDTD domain. Therefore, efficiency of the proposed

method is higher than the direct FDTD computations as long as small subdomains are simulated and the distance between them is sufficiently large.

**Conclusion:** The 3D FDTD algorithm on disjoint domains has been developed using the DGF formulation of this method. The developed method is more efficient than the direct FDTD computations as long as subdomains are small and the distance between them is sufficiently large. The developed 3D FDTD method on disjoint domains holds many applications for future work, such as simultaneous simulation of a transmitter and a receiver in radio communication systems. Moreover, this technique opens the doors for the development of new techniques of domain decomposition facilitating parallelisation of FDTD computations.

**Acknowledgments:** This work was realised within the HOMING PLUS Program of the Foundation for Polish Science, co-financed by the European Union Regional Development Fund.

© The Institution of Engineering and Technology 2013

22 December 2012

doi: 10.1049/el.2012.4462

T.P. Stefański (Gdansk University of Technology, Narutowicza 11/12, 80-233 Gdansk, Poland)

E-mail: tomasz.stefanski@pg.gda.pl

## References

- 1 Taflov, A., and Hangess, S.C.: 'Computational electrodynamics: the finite-difference time-domain method' (Artech House, Boston, MA, USA, 2005, 3rd edn)
- 2 Ma, W., Rayner, M.R., and Parini, C.G.: 'Discrete Green's function formulation of the FDTD method and its application in antenna modeling', *IEEE Trans. Antennas Propag.*, 2005, **53**, (1), pp. 339–346
- 3 de Hon, B.P., and Arnold, J.M.: 'Stable FDTD on disjoint domains - a discrete Green's function diakoptics approach'. Proc. 2007 European Conf. on Antennas and Propagation, (EuCAP 2007), Edinburgh, UK, November 2007, pp. 1–6
- 4 Merewether, D.E., Fisher, R., and Smith, F.W.: 'On implementing a numeric Huygens source scheme in a finite difference program to illuminate scattering bodies', *IEEE Trans. Nucl. Sci.*, 1980, **27**, (6), pp. 1829–1833
- 5 Stefanski, T.P., and Krzyzanowska, K.: 'Implementation of FDTD-compatible Green's function on graphics processing unit', *IEEE Antennas Wirel. Propag. Lett.*, 2012, **11**, pp. 1422–1425
- 6 Stefanski, T.P.: 'Accuracy of the discrete Green's function formulation of the FDTD method', *IEEE Trans. Antennas Propag.*, 2013, **61**, (2), (in print)